ISSN 0021-3640, JETP Letters, 2018, Vol. 107, No. 2, pp. 134–138. © Pleiades Publishing, Inc., 2018.
Original Russian Text © A.G. Smol'nikov, V.V. Ogloblichev, A.Yu. Germov, K.N. Mikhalev, A.F. Sadykov, Yu.V. Piskunov, A.P. Gerashchenko, A.Yu. Yakubovskii, M.A. Muflikhonova, S.N. Barilo, S.V. Shiryaev, 2018, published in Pis'ma v Zhurnal Eksperimental'noi i Teoreticheskoi Fiziki, 2018, Vol. 107, No. 2, pp. 134–138.

MISCELLANEOUS

Charge Distribution and Hyperfine Interactions in the $CuFeO_2$ Multiferroic According to ^{63,65}Cu NMR Data

A. G. Smol'nikov[a, *], V. V. Ogloblichev[a], A. Yu. Germov[a], K. N. Mikhalev[a], A. F. Sadykov[a], Yu. V. Piskunov[a], A. P. Gerashchenko[a], A. Yu. Yakubovskii[b], M. A. Muflikhonova[c], S. N. Barilo[d], and S. V. Shiryaev[d]

[a] *Mikheev Institute of Metal Physics, Ural Branch, Russian Academy of Sciences, Yekaterinburg, 620108 Russia*
[b] *National Research Center Kurchatov Institute, Moscow, 123182 Russia*
[c] *Ural Federal University, Yekaterinburg, 620002 Russia*
[d] *Institute of Solid State and Semiconductor Physics, National Academy of Sciences of the Republic of Belarus, Minsk, 220072 Republic of Belarus*
**e-mail: smolnikov@imp.uran.ru*

Received November 27, 2017; in final form, December 4, 2017

For the first time, the $CuFeO_2$ single crystal has been studied by ^{63,65}Cu nuclear magnetic resonance (NMR). The measurements have been carried out in the temperature range of $T = 100$–350 K in the magnetic field $H = 117$ kOe applied along different crystallographic directions. The components of the electric field gradient tensor and the hyperfine coupling constants are determined. It is shown that electrons of copper 4*s* and 3*d* orbitals are involved in the spin polarization transfer Fe $\rightarrow$ Cu. The occupancies of these orbitals are estimated.

DOI: 10.1134/S002136401802011X

1. INTRODUCTION

Research interest in $CuFeO_2$ delafossite is due to the presence of magnetoelectric effects in this system. The competition of exchange interactions in $CuFeO_2$ leads to spin frustration and the appearance of various magnetic structures, including those incommensurate with the lattice period. Simultaneously with the magnetic ordering in the fields of 60–130 kOe in this system, electric polarization is observed depending on an applied magnetic field [1–4].

In AMO_2 delafossites with identical magnetically active M^{3+} ions but different "nonmagnetic" A^+ ions, there are different types of magnetic ordering [5, 6], indicating the significant role of the A^+ ions in the exchange interactions and the appearance of electrical polarization.

The Cu^+ ions in the $CuFeO_2$ crystal structure are located between two neighboring planes of Fe^{3+} ions (Fig. 1). Using ^{63,65}Cu nuclei as NMR probes makes it possible to obtain information about the local charge symmetry and mechanisms of spin exchange between magnetic Fe^{3+} ions located in the neighboring planes.

2. SAMPLES AND EXPERIMENTAL PROCEDURE

The $CuFeO_2$ sample studied in this work was a $2\times2\times1$ mm single crystal prepared by the method described in [7]. The X-ray structural analysis of powder samples showed that $CuFeO_2$ has a hexagonal crystal structure with symmetry $R\bar{3}m$ and unit cell

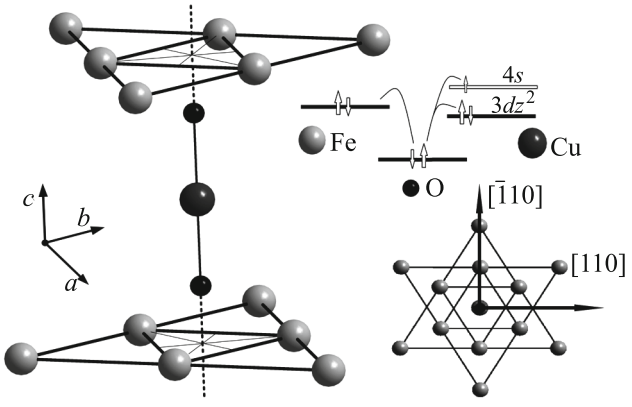

Fig. 1. Fragment of the crystal structure of $CuFeO_2$ in two projections and the spin-exchange scheme in the Fe–O–Cu chain.

parameters $a = 3.031(3)$ Å and $c = 17.162(6)$ Å at room temperature. These data are in agreement with the previously obtained results of structural studies [7].

Nuclear magnetic resonance measurements were performed on an Avance III 500 spectrometer (Bruker) with a superconducting solenoid $H =$ 117 kOe. In all experiments, the temperature was controlled with an accuracy of 0.5 K by two ITC 4/5 sensors (Oxford Instruments) placed in a cryostat and in the immediate vicinity of the sample. To exclude spurious signals from metallic copper, we used a resonance silver coil.

We obtained ^{63,65}Cu NMR spectra using the standard $\tau_{\pi/2} - t_{del} - \tau_{\pi} - t_{del}$ spin-echo technique. The duration of the first pulse was $\tau_{\pi/2} = 1$ μs and the power of the RF amplifier was 250–300 W. The repetition time of the experiment was 10 ms. When the spectra were wider than the frequency band excited by the RF pulse, the summation of the spectra recorded in the required frequency range with steps of 100 kHz was applied. The observation of the ^{63,65}Cu NMR signal in the paramagnetic phase of $CuFeO_2$ is complicated because of very short spin–spin relaxation times $T_2 \approx 5$ μs. Nevertheless, we observed the ^{63,65}Cu NMR in the studied compounds. Nuclear magnetic resonance spectra were measured with a delay between pulses $t_{del} = 8$ μs.

To calculate the shift of the NMR lines, we used a program for simulating spectra by numerically calculating the line shape based on the total Hamiltonian of the nuclear system, taking into account the Zeeman and quadrupole contributions [8–10].

To measure the susceptibility in the temperature range from 2 to 300 K in magnetic fields of 50 kOe, an MPMS SQUID magnetometer (Quantum Design, United States) was used. Measurements of magnetization were performed at the Collaborative Access Center, Mikheev Institute of Metal Physics.

3. EXPERIMENTAL RESULTS

Figure 2 shows NMR spectra of a single-crystal $CuFeO_2$ sample at $T = 300$ K in the external magnetic field $H = 117$ kOe applied along three orthogonal crystallographic directions. Spectra are two sets of lines, three lines in each. Such a structure of the spectra is due to the interaction of the quadrupole moment of ^{63}Cu and ^{65}Cu nuclei ($e^{63}Q = -0.220 \times 10^{-24}$ cm^2, $e^{65}Q = -0.195 \times 10^{-24}$ cm^2) with the electric field gradient (EFG) created at the location of the nuclei by their charge environment. In the presence of such interaction, three lines should be observed for nuclei with the spin $I = 3/2$: the central line corresponding to the $m_I = -1/2 \leftrightarrow 1/2$ transition and two satellites corresponding to the $m_I = -3/2 \leftrightarrow -1/2$ and $m_I = 1/2 \leftrightarrow 3/2$ transitions [11]. The difference between the resonance frequencies of the central line and satellites will be determined by the components of the EFG tensor V_{ij} ($i, j = x, y, z$). The EFG tensor is a symmetric second-rank tensor; in the system of principal axes, it has the diagonal form with three components $|V_{zz}| \geq |V_{yy}| \geq |V_{xx}|$. The orientation dependence of the NMR spectra obtained on a single crystal, in contrast to the powder spectra, makes it possible to determine not only the principal value V_{zz} of the EFG tensor and the asymmetry parameter $\eta = |(V_{xx} - V_{yy})|/V_{zz}$ but also the direction of the principal axes with respect to the crystal axes.

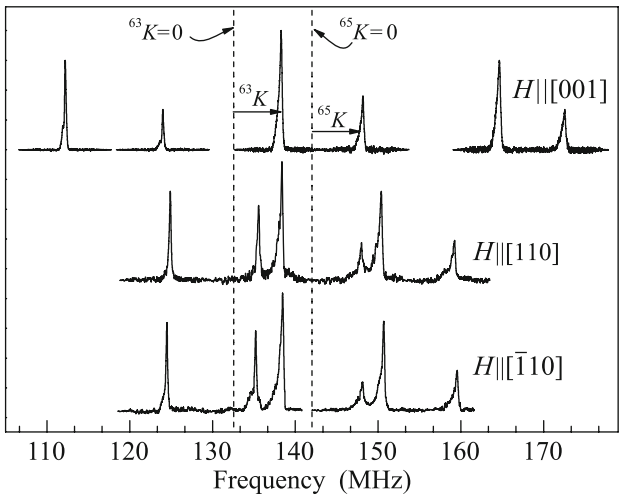

Fig. 2. ^{63,65}Cu NMR spectra obtained on a $CuFeO_2$ single-crystal sample at $T = 300$ K in the external magnetic field $H = 117$ kOe applied along three orthogonal crystallographic directions.

It is seen in Fig. 2 that the difference between the resonance frequencies of the central line and satellites in the direction of the field $H \parallel [001]$ is two times larger than that at $H \parallel [110]$ and $H \parallel [\bar{1}10]$; consequently, the tensor has axial symmetry $|V_{xx}| = |V_{yy}| = |0.5V_{zz}|$ with the asymmetry parameter $\eta \approx 0$. The principal axis of the EFG tensor is directed along the c axis of the crystal and determines the quadrupole frequency: $^{63}\nu_Q = V_{zz}e^{63}Q/2h = 26.6(1)$ MHz, $^{65}Q = V_{zz}e^{65}Q/2h = 23.6(1)$ MHz, where h is Planck's constant.

The behavior of the magnetic susceptibility $\chi(T)$ in the temperature range of 100–300 K is isotropic (does not depend on the orientation of the sample with respect to the direction of the external magnetic field) and is satisfactorily described by the Curie–Weiss law:

$$\chi(T) = \chi_0 + \chi_s(T) = \chi_0 + C/(T - \Theta), \qquad (1)$$

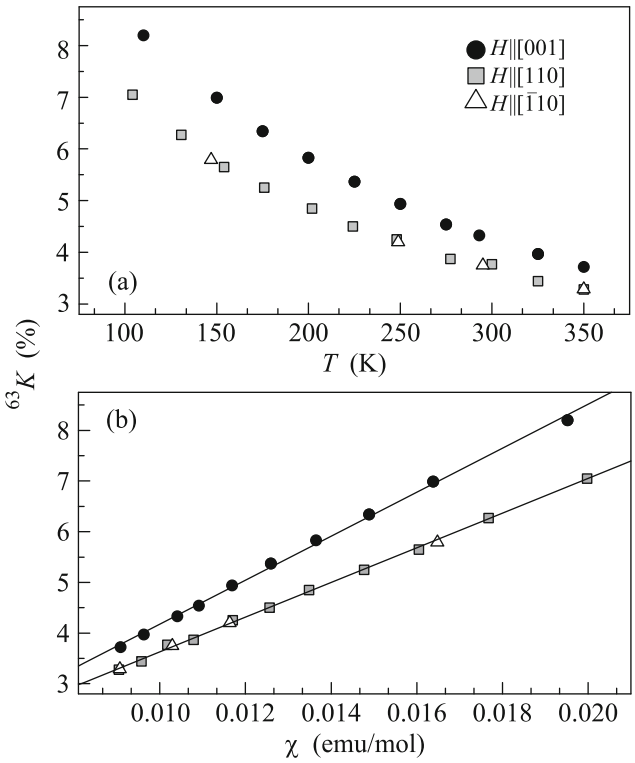

Fig. 3. Dependences (a) $^{63}K(T)$ and (b) $^{63}K(\chi)$ of the NMR line shift in the $CuFeO_2$ single crystal in the external field applied along three orthogonal crystallographic directions. Straight lines in (b) are approximations of the data.

where $C = 4.1(1)$ emu K/mol is the Curie constant, $\Theta = -99(3)$ K is the Weiss temperature, $\chi_0 = -7.0\times10^{-4}$ emu/mol, $\mu_{eff} = 5.8(1)\mu_B$, and μ_B is the Bohr magneton. The behavior of the magnetization changes sharply near $T_{N1} = 12.5$ K and $T_{N2} = 9$ K, indicating a magnetic phase transition with the establishment of the long-range magnetic order in the sample. All the data obtained are in good agreement with the results obtained in [2].

Figure 3a shows the temperature dependences of magnetic (with allowance for quadrupole corrections) shifts $K^\alpha(T)$ ($\alpha = [001]$, $[110]$, $[\bar{1}10]$) of the ^{63}Cu NMR line in the region of the paramagnetic state of $CuFeO_2$ ($T = 100$–350 K). The measurements of $K^\alpha(T)$ were performed on ^{63}Cu because of the higher natural content of this isotope (69% ^{63}Cu and 31% ^{65}Cu). The $K^\alpha(T)$ shifts are positive and their temperature dependences repeat the behavior of the magnetic susceptibility. The proportionality of the shifts and magnetic susceptibility is confirmed by K–χ Jaccarino–Clogston diagrams (Fig. 3b) [12].

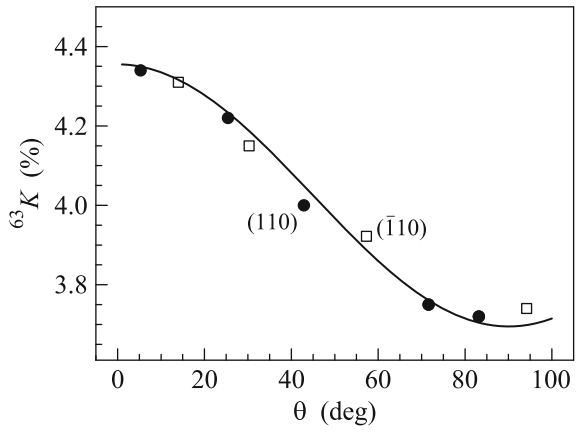

Fig. 4. Orientation dependence $^{63}K(\theta)$ in two crystallographic planes at $T = 300$ K, where θ is the angle between the direction of the external magnetic field and the c axis of the crystal. The line is the approximation of the data by Eq. (6).

The NMR line shift on the nonmagnetic ion nucleus, as well as the magnetic susceptibility, can be represented in the form

$$K^\alpha(T) = K_0^\alpha + K_s^\alpha(T). \quad (2)$$

The temperature-dependent spin contribution to the shift $K_s^\alpha(T)$ is proportional to the spin part of the susceptibility $\chi_s(T)$ and is determined by the hyperfine coupling constant A_{hf}^α:

$$K_s^\alpha(T) = \frac{A_{hf}^\alpha}{N_A\mu_B}\chi_s(T), \quad (3)$$

where N_A is the Avogadro number. Approximating $K^\alpha(\chi)$ by straight lines and using Eqs. (1)–(3), it is possible to determine A_{hf}^α and K_0^α [8, 9, 12]:

$$A_{hf}^{[001]} = 24.2\ \text{kOe}/\mu_B, \quad A_{hf}^{[110]} = A_{hf}^{[\bar{1}10]} = 19.1\ \text{kOe}/\mu_B,$$

$$K_0^{[001]} = K_0^{[110]} = K_0^{[\bar{1}10]} \approx 0.$$

It follows from these values that the hyperfine interaction on copper nuclei in $CuFeO_2$ is anisotropic. To determine the nature of the anisotropy of the hyperfine interaction, the orientation dependence $K(\theta)$ was analyzed at $T = 300$ K, where θ is the angle between the direction of the external magnetic field H and the c axis of the crystal (Fig. 4). The crystal was rotated in two planes $(\bar{1}10)$ and (110). For the most accurate determination of the direction of the external magnetic field H in relation to the crystal axes, we used the above parameters of the EFG tensor [13].

4. DISCUSSION

In the general case, the hyperfine coupling constant is determined by the sum of isotropic and anisotropic contributions:

$$A_{hf}^{\alpha} = A_{iso} + A_{ani}^{\alpha} = A_c + A_{cp} + A_{sd}^{\alpha} + A_{so}^{\alpha} + A_{dip}^{\alpha}, \quad (4)$$

where A_c and A_{cp} are the isotropic constants of the contact Fermi and core polarization hyperfine interactions, respectively, and A_{sd}^{α} and A_{so}^{α} are the anisotropic constants of the spin–dipole and spin–orbit hyperfine interactions with their own electrons, respectively. The constant of the dipole interaction of the nucleus with the magnetic moments of neighboring ions (A_{dip}^{α}) is also anisotropic.

The dipole coupling constants A_{dip}^{α} can be calculated [12]. The calculation gives the maximum value $A_{dip,max} = A_{dip}^{[001]} = 1.58(1)$ kOe/μ_B and $A_{dip}^{[110]} = A_{dip}^{[\bar{1}10]} = -0.79(1)$ kOe/μ_B. The Cu^+ ion in the $CuFeO_2$ crystal is located between two triangular lattices formed of magnetic Fe^{3+} ions (Fig. 1). Such magnetic environment leads to the orientation dependence of the dipole coupling constant described by the function

$$A_{dip}(\theta) = \frac{A_{dip}^{[001]}}{2}(3\cos^2(\theta) - 1), \quad (5)$$

where θ is the angle between the direction of the external magnetic field and the c axis of the crystal.

The A_{dip}^{α} values derived from the calculation are much less than the experimentally determined values of the hyperfine coupling constants A_{hf}^{α}. Consequently, the main contribution to A_{hf}^{α} is due to the transfer of the spin polarization from magnetic Fe^{3+} ions to Cu^+ ions.

The Fe^{3+} ions in $CuFeO_2$ are in the high-spin state and have five half-occupied $3d$ electron levels with total spin $S = 5/2$, and oxygen O^{2-} ions have the completely occupied $2s^2 2p^6$ orbitals (see Fig. 1) [14, 15]. Covalent Fe–O mixing involves only oxygen electrons with spin down ($\downarrow$), which will lead to the positive ($\uparrow$) spin polarization on O^{2-} ions, which, in turn, can be transferred to copper ions because of overlapping and covalent mixing of O $2s$, $2p$ orbitals and Cu $3d$, $4s$ orbitals. The positive spin polarization on the $3d$ orbital gives the isotropic negative contribution to the shift of the NMR line caused by A_{cp} and the anisotropic contributions from A_{sd} and A_{so}. However, the experiment indicates that $K > 0$; consequently, covalent O–Cu mixing should to some extent involve electrons in the copper $4s$ orbital. The nonzero positive spin density on the $4s$ orbital gives only the positive isotropic contribution to the NMR line shift owing to A_c. The participation of copper $4s$ and $3d$ orbitals in covalent mixing is a common case for compounds with monovalent copper Cu^+ [16–18].

As is seen in Fig. 4, the behavior of the shift does not depend on the choice of the direction of rotation of the crystal, and all the points lie on one plot of the corresponding function:

$$K(\theta) = A + B(3\cos^2(\theta) - 1), \quad (6)$$

where A and B are constants.

This behavior of the shift indicates a purely dipole nature of A_{ani}^{α} ($A_{so}^{\alpha} \approx 0$), which makes it possible to separate the isotropic and anisotropic parts of the hyperfine coupling constant. In fact, it was shown in [19, 20] that covalent O–Cu mixing involves electrons of the copper $3d_z^2$ orbital whose z axis is directed along the c axis of the crystal. In this case, the spin polarization of the $3d_z^2$ orbital creates the spin–dipole field, for which $A_{sd}^{[001]} = -2A_{sd}^{[110]} = -2A_{sd}^{[\bar{1}10]}$. Then, it follows from Eq. (4) that $A_{iso} = \frac{1}{3}(A_{hf}^{[001]} + 2A_{hf}^{[110]}) = 20.8$ kOe/μ_B, $A_{ani}^{[001]} = 3.4$ kOe/μ_B, and $A_{ani}^{[110]} = A_{ani}^{[\bar{1}10]} = -1.7$ kOe/μ_B. Further, using the A_{dip}^{α} value, we find $A_{sd}^{[100]} = 1.8$ kOe/μ_B and $A_{sd}^{[110]} = A_{sd}^{[\bar{1}10]} = -0.9$ kOe/μ_B. The hyperfine coupling constants A_{sd}^{α} depend on the occupancy of the $3d_z^2$ orbital $n(3d) = (n\uparrow - n\downarrow)$ and the average radius of the orbit $\langle r^{-3}\rangle$ as [15]

$$A_{sd}^{[100]} = \frac{4}{7}n(3d)\mu_B\langle r^{-3}\rangle;$$
$$A_{sd}^{[110]} = A_{sd}^{[\bar{1}10]} = -\frac{2}{7}n(3d)\mu_B\langle r^{-3}\rangle. \quad (7)$$

Using the value $\langle r^{-3}\rangle = 5.1\times10^{25}$ cm^{-3} calculated for the free ion [21], we estimate $n(3d) = 0.007$.

The hyperfine coupling constant of the core polarization is determined by the expression $A_{cp} = n(3d)A_{cp}^{eff} = -0.9$ kOe/μ_B, where $A_{cp}^{eff} = -125$ kOe/μ_B is the field created on the nucleus by one electron (hole) on the $3d$ orbital [22]. The known A_{cp} and A_{iso} values make it possible to determine the contact Fermi hyperfine coupling constant A_c. Using the expression $A_c = n(4s)A_c^{eff} = 21.7$ kOe/μ_B, where $A_c^{eff} = 2$ MOe/μ_B is the field on the nucleus from one electron on the $4s$ orbital [20], we estimate the occupancy of the $4s$ orbital as $n(4s) = 0.01$. The estimates of hyperfine coupling constants and occupancies of copper $3d$ and $4s$ orbitals are given in Table 1.

Table 1. Hyperfine coupling constants and the occupancy degree on copper 4*s* and $3d_z^2$ orbitals in $CuFeO_2$

A_c (kOe/μ_B)	A_{cp} (kOe/μ_B)	A_{so} (kOe/μ_B)	A_{sd}^c (kOe/μ_B)	A_{sd}^{ab} (kOe/μ_B)	A_{dip}^c (kOe/μ_B)	A_{dip}^{ab} (kOe/μ_B)	$n(3d)$ (%)	$n(4s)$ (%)
21.7	−0.9	0	1.8	−0.9	1.6	−0.8	0.7	1

5. CONCLUSIONS

It has been shown that the EFG tensor on copper positions in $CuFeO_2$ has axial symmetry $\eta \approx 0$; the principal axis of the EFG tensor is directed along the *c* axis of the crystal. The quadrupole frequencies for two copper isotopes have been determined: $^{63}\nu_Q$ = 26.6(1) MHz, $^{65}\nu_Q$ = 23.6(1) MHz.

The nature of hyperfine fields on nuclei copper has been determined by jointly analyzing the orientation and temperature dependences of the magnetic shift of ^{63}Cu NMR lines and magnetic susceptibility data. It has been established that electrons of the copper 4*s* and 3*d* orbitals are involved in the O–Cu covalent mixing and the occupancies of these orbitals have been estimated.

We are grateful to S.V. Verkhovskii for the productive discussion of experimental results. This study was supported by the Russian Science Foundation (project no. 16-12-10514).

REFERENCES

1. T. Kimura, J. C. Lashley, and A. P. Ramirez, Phys. Rev. B **73**, 220401 (2006).
2. O. A. Petrenko, M. R. Lees, G. Balakrishnan, S. de Brion, and G. Chouteau, J. Phys.: Condens. Matter **17**, 2741 (2005).
3. F. Ye, Y. Ren, Q. Huang, J. A. Fernandez-Baca, Pengcheng Dai, J. W. Lynn, and T. Kimura, Phys. Rev. B **73**, 220404R (2006).
4. T. Nakajima, S. Mitsuda, K. Takahashi, M. Yamano, K. Masuda, and H. Yamazaki, Phys. Rev. B **79**, 214423 (2009).
5. N. Terada, D. Khalyavin, P. Manuel, Y. Tsujimoto, and A. Belik, Phys. Rev. B **91**, 094434 (2015).
6. A. Sobolev, V. Rusakov, A. Moskvin, A. Gapochka, A. Belik, I. Glazkova, A. Akulenko, G. Demazeau, and I. Presniakov, J. Phys.: Condens. Matter **29**, 275803 (2017).
7. P. Dordor, J. P. Chaminade, A. Wichainchai, E. Marquestaut, J. P. Doumerc, M. Pouchard, P. Hagenmuller, and A. Ammar, J. Solid State Chem. **75**, 105 (1988).
8. A. F. Sadykov, A. P. Gerashchenko, Yu. V. Piskunov, V. Ogloblichev, A. Smol'nikov, S. Verkhovskii, A. Yakubovskii, E. Tishchenko, and A. Bush, J. Exp. Theor. Phys. **115**, 666 (2012).
9. A. G. Smol'nikov, V. V. Ogloblichev, S. V. Verkhovskii, K. N. Mikhalev, A. Yu. Yakubovskii, Y. Furukawa, Yu. V. Piskunov, A. F. Sadykov, S. N. Barilo, and S. V. Shiryaev, Phys. Met. Metallogr. **118**, 134 (2017).
10. A. G. Smol'nikov, V. V. Ogloblichev, S. V. Verkhovskii, K. N. Mikhalev, A. Yu. Yakubovskii, K. Kumagai, Y. Furukawa, A. F. Sadykov, Yu. V. Piskunov, A. P. Gerashchenko, S. N. Barilo, and S. V. Shiryaev, JETP Lett. **102**, 674 (2015).
11. A. Abragam, *The Principles of Nuclear Magnetism* (Clarendon, Oxford, 1961).
12. A. M. Clogston, V. Jaccarino, and Y. Yafet, Phys. Rev. **134**, A650 (1964).
13. A. G. Smol'nikov, V. V. Ogloblichev, and A. F. Sadykov, J. Exp. Theor. Phys. **112**, 1020 (2011).
14. V. R. Galakhov, A. I. Poteryaev, E. Z. Kurmaev, and V. I. Anisimov, Phys. Rev. B **56**, 4584 (1997).
15. A. Abragam and B. Bleaney, *Electron Paramagnetic Resonance of Transition Ions* (Clarendon, Oxford, 1970).
16. T. Yokobori, M. Okawa, K. Konishi, R. Takei, K. Katayama, S. Oozono, T. Shinmura, T. Okuda, H. Wadati, E. Sakai, K. Ono, H. Kumigashira, M. Oshima, T. Sugiyama, E. Ikenaga, N. Hamada, and T. Saitoh, Phys. Rev. B **87**, 195124 (2013).
17. J. M. Zuo, M. Kim, M. O'Keeffe, and J. C. H. Spence, Nature (London, U.K.) **401**, 49 (1999).
18. J. Ghijsen, L. H. Tjeng, H. Eskes, and G. A. Sawatzky, Phys. Rev. B **42**, 2268 (1990).
19. H. Hiraga, T. Makino, T. Fukumura, H. Weng, and M. Kawasaki, Phys. Rev. B **42**, 041411 (R) (2011).
20. W. Ketir, S. Saadi, and M. Trari, J. Solid State Electrochem. **16**, 213 (2012).
21. A. J. Freeman and R. E. Watson, in *Magnetism IIA,* Ed. by G. T. Rado and H. Suhl (Academic, New York, 1965), p. 291.
22. F. Mila and T. M. Rice, Physica C **157**, 561 (1989).

Translated by L. Mosina